Filip Kutt, Michał Michna, Mieczysław Ronkowski, Piotr J. Chrzan
Gdansk University of Technology
Faculty of Electrical and Control Engineering

POLYARMONIC MODEL OF SYNCHRONOUS GENERATOR FOR ANALYSIS OF AUTONOMOUS POWER GENERATION SYSTEMS

Abstract: This paper presents the polyharmonic modelling of synchronous generator (SG) in machine variables. The simple geometry and windings physical layout has been used for inductance calculations of a salient-pole SG. The main advantage of this model is the ease of describing an autonomous power generation system (APGS) in terms of its topology and thus providing effective analysis at the static and dynamic states, both for normal and fault operations. Particularly, the model can be used to obtain SG voltage and currents for their more extensive harmonic analysis. Comparison of the simulation and measurement results has shown their good agreement, i.e., validating the elaborated polyharmonic model of SG.

1. Introduction

Development of autonomous power generation systems (APGS), i.e., from more electric aircraft/vehicle systems to combined heat and electric power generation systems (micro-CHP), are a fast growing branch of research and industry activates [3, 8, 9]. The demand for power in these systems is growing along with expectations for their reliability and efficiency. One of the most important elements of APGS is the synchronous generator (SG) which can operate in different network topologies – with or without grounded neutral point. Also an asymmetric load may be often applied to the SG. An accurate and computer efficiency model is required to analyze the static and dynamic behaviour of the SG [4, 5, 6, 7, 11]. Particularly, a polyharmonic model in machine variables have to be used to obtain SG voltage and currents for their more extensive harmonic analysis [2].
This paper presents the polyharmonic modelling of SG in machine variables. Winding function approach presented earlier by previous researchers [1, 4, 10, 12] has been modified and expressed in general form to account the magnetomotive force (MMF) space harmonics for developing expressions for self- and mutual inductance calculations.

2. Polyharmonic model of synchronous generator in machine variables

2.1 General equations

An elementary two-pole, salient-pole synchronous machine shown in Fig.1 will be used for developing a polyharmonic model of SG in machine variables.

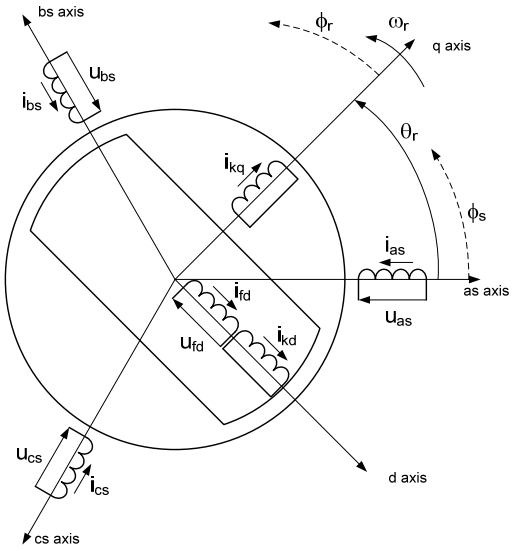

Figure 1. Physical description of two-pole salient-pole synchronous generator with hybrid reference frames: axes as, bs and cs fixed in stator; axes q and d fixed in rotor

The stator windings (denoted by *as*, *bs, cs*) are symmetrical and placed at the magnetic axes *as*, *bs* and *cs* displaced by 120 degrees, respectively. The rotor is equipped with a field winding (denoted by *fd*), and two damper windings (denoted by *kq* and *kd*) placed at magnetic axes *d* and *q* are at right angle, respectively.
Using the notation elaborated by P.C. Krause [4] the voltage equations of SG in vector-matrix form are following:

$$\mathbf{u}_{abcs} = -\mathbf{r}_s \mathbf{i}_{abcs} + \frac{\mathrm{d}\boldsymbol{\lambda}_{abcs}}{\mathrm{d}t} \tag{1}$$

$$\mathbf{u}_{qdr} = \mathbf{r}_r \mathbf{i}_{qdr} + \frac{\mathrm{d}\boldsymbol{\lambda}_{qdr}}{\mathrm{d}t} \tag{2}$$

where $\mathbf{r}_s$, $\mathbf{r}_r$ are the diagonal matrices of the stator and rotor winding resistances, $\mathbf{i}_{abcs}$ and $\mathbf{r}_{qdr}$ are the vectors of the stator and rotor currents, respectively.
The flux linkage vectors $\boldsymbol{\lambda}_{abcs}$ and $\boldsymbol{\lambda}_{qdr}$ in the equations (1) and (2) are following:

$$\begin{bmatrix}\boldsymbol{\lambda}_{abcs}\\ \boldsymbol{\lambda}_{qdr}\end{bmatrix}=\begin{bmatrix}\mathbf{L}_s(\theta_r) & \mathbf{L}_{sr}(\theta_r)\\ (\mathbf{L}_{sr}(\theta_r))^T & \mathbf{L}_r\end{bmatrix}\begin{bmatrix}-\mathbf{i}_{abcs}\\ \mathbf{i}_{qdr}\end{bmatrix} \tag{3}$$

In equations (3) the matrices denote:
$\mathbf{L}_s$ is the stator windings self and mutual inductance

$$\mathbf{L}_s=\begin{bmatrix}L_{asas}(\theta_r) & L_{asbs}(\theta_r) & L_{ascs}(\theta_r)\\ L_{asbs}(\theta_r) & L_{bsbs}(\theta_r) & L_{bscs}(\theta_r)\\ L_{ascs}(\theta_r) & L_{bscs}(\theta_r) & L_{\mathrm{csc}s}(\theta_r)\end{bmatrix}, \tag{4}$$

$\mathbf{L}_r$ is the rotor windings (field and damper cages) self and mutual inductance

$$\underline{\mathbf{L}}_r=\begin{bmatrix}L_{kqkq} & 0 & 0\\ 0 & L_{fdfd} & L_{fdkd}\\ 0 & L_{kdfd} & L_{kdkd}\end{bmatrix} \tag{5}$$

$\mathbf{L}_{sr}$ is the mutual inductance between stator and rotor windings

$$\mathbf{L}_{sr}=\begin{bmatrix}L_{askq}(\theta_r) & L_{asfd}(\theta_r) & L_{askd}(\theta_r)\\ L_{bskq}(\theta_r) & L_{bsfd}(\theta_r) & L_{bskd}(\theta_r)\\ L_{cskq}(\theta_r) & L_{csfd}(\theta_r) & L_{cskd}(\theta_r)\end{bmatrix} \tag{6}$$

where θ_r is the electrical angular displacement of the rotor, the subscripts s, r, f and k denote stator, rotor, field and cage windings, respectively.
The electromagnetic torque in terms of the energy stored in the coupling field

$$T_e=\left(\frac{P}{2}\right)\frac{\partial W_c(\mathbf{i}_{abcs},\mathbf{i}_{qdr},\mathbf{L}_s,\mathbf{L}_{sr},\mathbf{L}_r)}{\partial\theta_r} \tag{7}$$

The torque and rotor speed are related by:

$$T_e=-J\frac{\mathrm{d}\omega_{rm}}{\mathrm{d}t}-B_m\omega_{rm}+T_l \tag{8}$$

where J is the inertia expressed in kg.m^2, B_m friction coefficient, ω_{rm} mechanical angular speed of the rotor, ω_r electrical angular speed of the rotor. They related by

$$\omega_r=\frac{\mathrm{d}\theta_r}{\mathrm{d}t}\ \text{and}\ \omega_r=\left(\frac{P}{2}\right)\omega_{rm}$$

where P is the number of poles.

The input torque T_l is positive for a torque input to the shaft of the SG.

2.2 Inductance matrices

The following assumptions to simplify the SG model are assumed: (i) only the first and third space harmonics of stator and rotor windings MMF are considered, (ii) saturation of magnetic circuits is neglected.
For the modelling it is assumed that the air-gap length variation may be approximated as [4]:

$$\delta(\phi_s-\theta_r)=\frac{1}{\alpha}\cdot\frac{1}{\alpha_1'-\alpha_2'\cos(2(\phi_s-\theta_r))} \tag{9}$$

where ϕ_s is the angular displacement of the stator (Fig.1), α is the absolute value (in meters) of the air-gap length along d axis, the relative value of α is expressed as $\frac{1}{\alpha}=\frac{1}{\alpha_1+\alpha_2}$ while the minimum air-gap length is $\frac{1}{\alpha_1+\alpha_2}$ and the maximum is $\frac{1}{\alpha_1-\alpha_2}$, the relative values of α_1' and α_2' are expressed as $\alpha_1'=\frac{\alpha_1}{\alpha}$ and $\alpha_2'=\frac{\alpha_2}{\alpha}$.

The MMF of the stator winding is defined as:

$$MMF_{as}(\phi_s,t)=\\ =\frac{N_s'}{2}i_{as}(t)(\cos(\phi_s)+A_{3s}'\cos(3\phi_s)) \tag{10}$$

where N'_s represents the number of turns of the equivalent sinusoidally distributed stator winding, A'_{3s} is relative value of the third harmonic amplitude of stator winding MMF expressed as $A_{3s}'=A_{3s}/A_{1s}$ (A_{1s} and A_{3s} are absolute values of the MMF amplitudes of the first and third harmonic, respectively). Similar expressions as (10) are defined for other stator phases taking into account that their magnetic axes are displaced by 120^o with respect to each other, respectively.
The MMF of field winding is defined as:

$$MMF_{fd}(\phi_r,t)=\\ =-\frac{N_{fd}'}{2}i_{fd}(t)(\sin(\phi_r)+A_{3fd}'\sin(3\phi_r)) \tag{11}$$

where N'_{fd} represents the number of turns of the equivalent sinusoidally distributed field winding, ϕ_r is the angular displacement of the rotor (Fig.1), A'_{3fd} is relative value of the third harmonic amplitude of field winding MMF

expressed as $A'_{3fd} = A_{3fd} / A_{1fd}$ (A_{1fd} and A_{3fd} are absolute values of the MMF amplitudes of the first and third harmonic, respectively). Similar expressions as (11) are defined for the cage windings *kq* and *kd* taking into account that their magnetic axes are displaced by 90° with respect to each other, respectively.

The equations (10) and (11) are right for the stator and field winding space distributions expressed as following:

$$N_{as}(\phi_s) = \frac{1}{i_{as}(t)}\left(\frac{\mathrm{d}}{\mathrm{d}\phi_s} MMF_{as}(\phi_s, t)\right) \tag{12a}$$

$$N_{fd}(\phi_r) = \frac{1}{i_{fd}(t)}\left(\frac{\mathrm{d}}{\mathrm{d}\phi_r} MMF_{fd}(\phi_r, t)\right) \tag{12b}$$

Substituting equation (10) and (11) into (12a) and (12b), respectively, yields:

$$N_{as}(\phi_s) = -\frac{N'_s}{2}\left(\sin(\phi_s) + 3A'_{3s}\sin(3\phi_s)\right) \tag{13}$$

$$N_{fd}(\phi_r) = -\frac{N'_{fd}}{2}\left(\cos(\phi_r) + 3A'_{3fd}\cos(3\phi_r)\right) \tag{14}$$

Taking into account the above consideration, the following expressions for calculating the SG stator and field winding self and mutual inductances can be developed, respectively, as following:

$$L_{asas}(\theta_r) = L_{ls} + \frac{1}{i_{as}(t)} \times \int_{\pi}^{2\pi}\left[N_{as}(\phi_s) \times \int_{\phi_s}^{\phi_s+\pi}\left[\mu_0 \frac{1}{\delta(\xi-\theta_r)} MMF_{as}(\xi, t) rl\right]\mathrm{d}\xi\right]\mathrm{d}\phi_s \tag{15a}$$

$$L_{asfd}(\theta_r) = \frac{1}{i_{fd}(t)} \times \int_{\pi}^{2\pi}\left[N_{as}(\phi_s) \times \int_{\phi_s}^{\phi_s+\pi}\left[\mu_0 \frac{1}{\delta(\xi-\theta_r)} MMF_{fd}(\xi, t) rl\right]\mathrm{d}\xi\right]\mathrm{d}\phi_s \tag{15b}$$

$$L_{fdfd} = L_{lfd} + \frac{1}{i_{fd}(t)} \times \int_{\pi/2}^{3\pi/2}\left[N_{fd}(\phi_r) \times \int_{\phi_r}^{\phi_r+\pi}\left[\mu_0 \frac{1}{\delta(\xi)} MMF_{fd}(\xi, t) rl\right]\mathrm{d}\xi\right]\mathrm{d}\phi_r \tag{15c}$$

where *l* is the axial length of the air-gap of the machine and *r* is the mean radius of the air-gap, and ξ is dummy variable, the subscript *l* denote leakage inductance. Similar expressions as (15) are defined for other self- and mutual inductances of the matrices (4), (5) and (6), respectively.

For further model development it is assumed that the first harmonic amplitudes of self and mutual winding inductances, associated with the air-gap field, may be expressed as following:

$$L_s = \left(\frac{N'_s}{2}\right)^2 \Lambda \tag{16}$$

$$L_{sfd} = \left(\frac{N'_s}{2}\right)\left(\frac{N'_{fd}}{2}\right)\Lambda \tag{17}$$

$$L_{fd} = \left(\frac{N'_{fd}}{2}\right)^2 \Lambda \tag{18}$$

where $\Lambda = rl\pi\mu_0\alpha$ is the magnetic permeance of the air-gap. Similar expressions as (15) – (18) are defined for self- and mutual inductances of the cage windings *kq* and *kd*, respectively.

The final expressions for calculating the winding inductances are following:

$$L_{asas}(\theta_r) = L_{ls} + L_s\left(\begin{array}{l}\left(1 + A'^2_{3s}\right)\alpha'_1 - \\ \left(\frac{1}{2} + A'_{3s}\right)\alpha'_2\cos(2\theta_r)\end{array}\right) \tag{19}$$

$$L_{asbs}(\theta_r) = -\frac{1}{2}L_s \times \left(\left(1 - 2A'^2_{3s}\right)\alpha'_1 + \left(1 - A'_{3s}\right)\alpha'_2\cos\left(2\left(\theta_r - \frac{\pi}{3}\right)\right)\right) \tag{20}$$

$$L_{asfd}(\theta_r) = L_{sfd}\left(\begin{array}{l}\left(\alpha'_1 + \left(1 - A'_{3fd}\right)\frac{\alpha'_2}{2}\right)\sin(\theta_r) + \\ \left(A'_{3s}\left(\alpha'_1 A'_{3fd} - \frac{\alpha'_2}{2}\right)\right)\sin(3\theta_r)\end{array}\right) \tag{21}$$

$$L_{fdfd} = L_{lfd} + L_{fd}\left(\begin{array}{l}\left(1 + A'^2_{3fd}\right)\alpha'_1 + \\ \left(\frac{1}{2} - A'_{3fd}\right)\alpha'_2\end{array}\right) \tag{22}$$

Similar expressions as (19) – (22) are developed for other stator phases and field winding, respectively.

3. Simulation and measurement

The developed SG polyharmonic model has been verified for a 10 kVA, 3-phase and salient-poles machine (data given in the appendix).

The MMF distributions of the stator winding (Fig.2) and field winding (Fig.3) have been calculated using the SG manufactured data sheet.

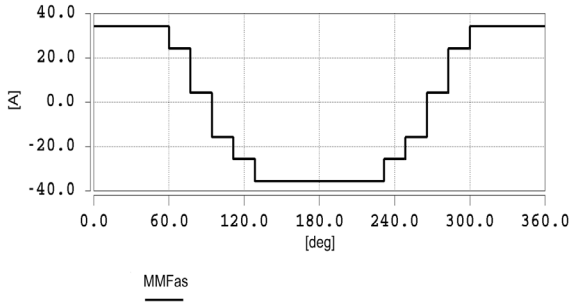

Figure 2. Plot of the air-gap MMF due to the as stator winding with the assumption that i_{as}=1 A

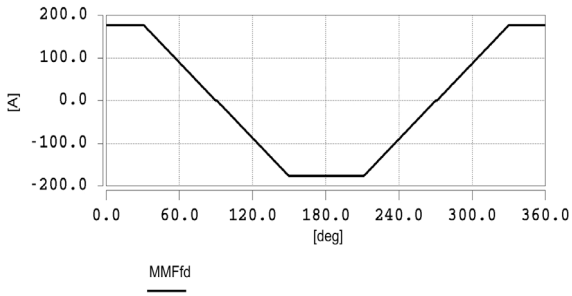

Figure 3. Plot of the air-gap MMF due to the fd winding with the assumption that i_{fd}=1 A

Having determined the stator MMF (Fig.2) and field MMF (Fig.3) plots the harmonic coefficients A'_{3s} and A'_{3fd} have been calculated. To determine the coefficients α'_1, α'_2 the SG EMF e_0 has been measured as a function of time and the harmonic analysis has been carried out (Fig.4) using Mathematica software.

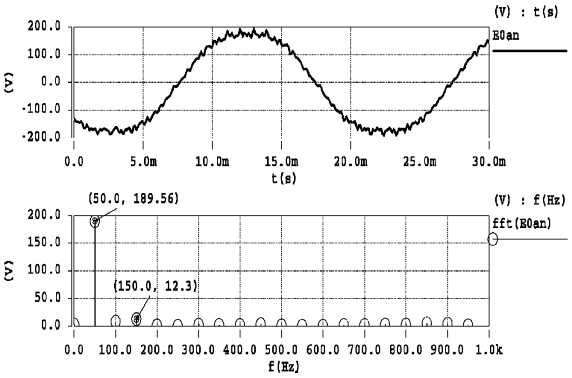

Figure 4. Measured EMF wave (above) and its harmonic analysis (below)

The instantaneous value of EMF e_{0as} can be expressed:

$$e_{0as} = -\frac{d\psi_{as}}{dt} = -i_{fd}\frac{\partial L_{asfd}(\theta_r)}{\partial \theta_r}\omega_r \qquad (23)$$

Substituting the equation (21) into (23) yields the following expressions for the amplitudes of first E_{01as} and third E_{03as} EMF harmonics (phase values for *as* winding), respectively:

$$E_{0an1h} = -i_{fd}\omega_r L_{sfd}\left(\alpha'_1 + \left(1 - A'_{3fd}\right)\frac{\alpha'_2}{2}\right) \qquad (24)$$

$$E_{0an3h} = -i_{fd}\omega_r L_{sfd}\,3\left(A'_{3s}\left(\alpha'_1 A'_{3fd} - \frac{\alpha'_2}{2}\right)\right) \qquad (25)$$

Using the equations (24) and (25) the values of the air-gap coefficients α'_1 and α'_2 have been determined.

For the considered SG a steady-state analysis at constant rotor speed have been carried out for no-load and load tests.

Two SG simulation models – monoharmonic (MHM) and polyharmonic (PHM) – have been elaborated using the MAST language of the Synopsys/Saber simulator [7].

A simulation schematic of the SG model elaborated using the Synopsys/Saber Sketch software is shown in Fig. 5. Under the symbol "ELMOR GCe64a" is denoted the SG model. The "inside" of this model contains adequate equations and formulae presented in section 2.

Chosen simulation and measurement results are shown in Fig.6 – Fig.9. The constant angular speed operation of the SG has been assumed. The SG has been loaded by resistive load providing approximately 45% of the rated load. The neutral point of the SG and the load has been connected and grounded.

The measurement results have shown that there is a relatively large third harmonic component in the stator voltage and current, i.e., the third harmonic have a significant influence on the shapes of the voltage and current waves of the studied SG. The simulation results have shown that the influence of the third harmonic component is relatively smaller when comparing with the measurement results. Moreover, the measurements have shown that the relative value of third harmonic component of the stator voltage has increased from 8% to 23% for no-load and rating load, respectively. From the simulations it follows that the third harmonic component has decreased from 8% to 6.4%, respectively.

It has to be noticed that a relatively greater difference between the measured and simulation results are for the third harmonic component of the neutral wire current of the SG (Fig.9).

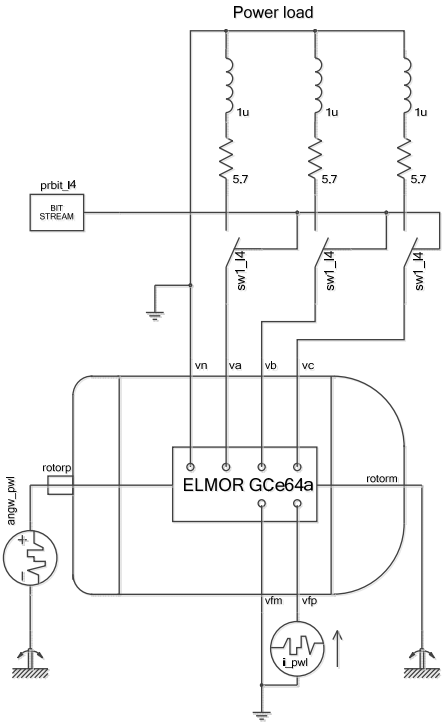

Figure 5. Simulation schematic of the SG model elaborated using the Synopsys/Saber Sketch software

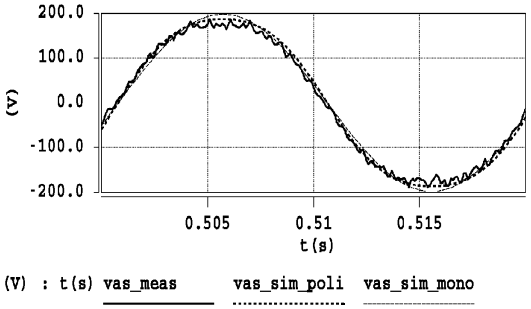

Figure 6. EMF of the SG at no-load: vas_meas – measurement, vas_sim_poli – PHM simulation, vas_sim_mono – MHM simulation

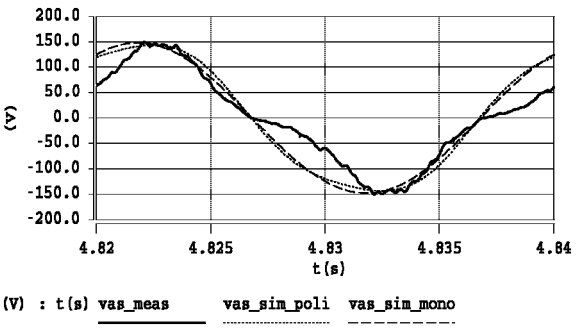

Figure 7. Stator voltage (phase to neutral) of the SG at load: vas_meas – measurement, vas_sim_poli – PHM simulation, vas_sim_mono – MHM simulation

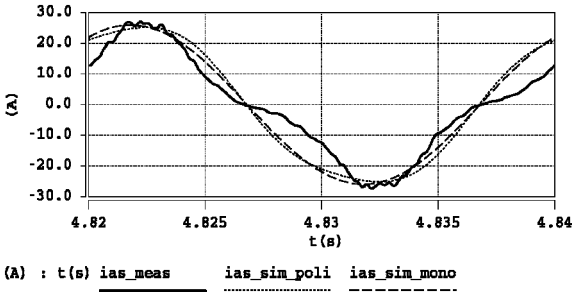

Figure 8. Stator current of the SG at load: ias_meas – measurement, ias_sim_poli – PHM simulation, ias_sim_mono – MHM simulation

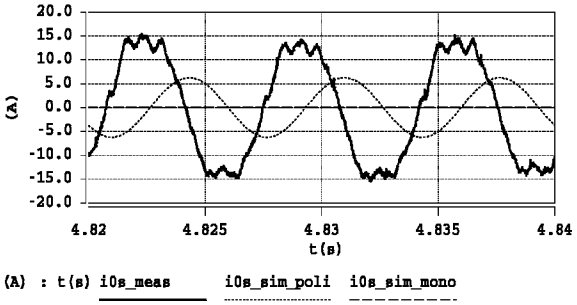

Figure 9. Neutral wire current at load: i0s_meas – measurement, i0s_sim_poli – PHM simulation, i0s_sim_mono – MHM simulation

While comparing the measured and simulation results it has to be noticed that for the simulation model of the considered SG the third harmonic component has been taken into account only for the mutual inductance L_{asfd}. Neglecting this component for the other inductances has an influence on the accuracy of the simulation model. Moreover, assuming linear magnetic circuit also decreases the accuracy of the developed model.

The comparison of the measured and simulation results of the studied SG for other load characters (pure reactive and mixed) will be presented at the conference.

4. Conclusions

In this paper, the simple geometry and windings physical layout has been used for inductance calculations of a salient-pole synchronous SG. Winding function approach presented earlier by previous researchers has been modified and expressed in general form to account the MMF space harmonics for developing expressions for self- and mutual inductance calculations. SG equations in terms of machine variables were obtained using the coupled magnetic circuit approach and simple geometry and windings physical layout.

The developed linear polyharmonic model of the SG exhibit a network with the same number of external terminals/ports as the real machine, and represents its behaviour in terms of the electrical (stator and rotor windings) and mechanical (shaft) variables as well. The main advantage of this model is the ease of describing APGS in terms of its topology and thus providing effective analysis at the static and dynamic states, both for normal and fault operations. Particularly, the model can be used to obtain SG voltage and currents for their more extensive harmonic analysis.
Experiments have been conducted on a salient-pole SG and the results were found to be in a close agreement to the simulation results.

5. References

[1] Al-Nuaim N.A., Toliyat H. A.: *A novel method for modeling dynamic air-gap eccentricity in synchronous machines based on modified winding function theory*, IEEE Trans. Energy Con. Vol.13, Issue 2, 1998.
[2] Eleschova Z., Belan A., Mucha M.: *Harmonic distortion produced by synchronous generator in thermal -power plant*, Proc. of the 6th WSEAS Inter. Conf. on Power Systems, 2006.
[3] Gieras J.F.: *Advancements in electric machines*, Heidelberg, Springer 2009.
[4] Krause P. C.: *Analysis of electric machinery*, McGraw-Hill Book Company, 1986.
[5] Kudła J.: *Modele matematyczne maszyn elektrycznych prądu przemiennego uwzględniające nasycenie magnetyczne rdzeni.* Z N Pol. Śląskiej, Nr 1683, Gliwie 2005.
[6] Kutt F., Michna M., Chrzan P. J., Ronkowski M.: *Nonlinear model of a synchronous generator for analysis of more electric aircraft power systems,* SME 2009.
[7] Michna M., Kutt F., Chrzan P. J., Ronkowski M.: *Modeling and analysis of a synchronous generator in more electric aircraft power system using Synopsys/Saber simulator,* Proc. Inter. XVI Sym. Micromachines & Servosystems, MiS 2008.
[8] Moir I., Seabridge A.: *Aircraft Systems: Mechanical, electrical, and avionics subsystems integration,* John Wiley & Sons 2008.
[9] Predd P. P.: *A power plant for the home*, IEEE Spectrum, April 2007.
[10] Sobczyk T.: *Metodyczne aspekty modelowania matematycznego maszyn indukcyjnych*, WNT, Warszawa, 2004.
[11] Tantawy A., Koutsoukos X., Biswas G.: *Aircraft AC generators: Hybrid system modeling and simulation*, Inter. Conf. on Prognostics and Health Management, 2008.
[12] Toliyat H. A., Al-Nuaim N.A.: *Simulation and detection of dynamic air-gap eccentricity in salient-pole synchronous machines*, IEEE Trans. on Industry Applications, January/February 1999.

Acknowledgment

This material is based in part upon work supported by the Ministry of Science and Higher Education in Poland under grant N N510 328937 for the years of 2009 – 2011.
The authors would like to express their gratitude to CI TASK for provided Wolfram Mathematica software.

Appendix

Synchronous generator parameters: type GCe64a (manufactured by ELMOR), 10 kVA, 231 V (Y), 0.8 pf, 4-pole, 1500 rpm, l = 130 mm, r = 194.6 mm, α = 0.8 mm, 42 stator slots,
N_s = 70 turns/phase, 9 pitch, r_s = 0.33 Ω,
N_{fd} = 177 turns/pole, r_{fd} = 2.25 Ω.

Authors

Filip Kutt, M.Sc., Eng., PhD student, tel. +(48-58) 3472077, fax: +(48-58) 3471939, e-mail: f.kutt@ely.pg.gda.pl. The author is a scholar within Sub-measure 8.2.2 Regional Innovation Strategies, Measure 8.2 Transfer of knowledge, Priority VIII Regional human resources for the economy Human Capital Operational Prog. co-financed by EU Social Fund and state budget.

Michał Michna, Ph.D., Eng., tel. +(48-58) 3472979, fax: +(48-58) 3410880, e-mail: m.michna@ely.pg.gda.pl

Mieczysław Ronkowski, Ph.D., D.Sc., Eng., associate prof., Gdansk University of Technology, tel. +(48-58) 3472087, fax: +(48-58) 3410880, e-mail: m.ronkowski@ely.pg.gda.pl.

Piotr Chrzan, Ph.D., D.Sc., Eng., tel. +(48-58) 342534, fax: +(48-58)3410880, e-mail: p.chrzan@ely.pg.gda.pl

The authors are employed at the Gdansk University of Technology, Narutowicza 11/12, 80-233 Gdańsk, Poland.

Recenzent

Prof. dr hab. inż. Tadeusz Sobczyk